

Chapter 2

Experimental Study: Damage Detection Method for Weld Fracture of Beam-Column Connections in Steel Moment-Resisting-Frame Buildings

Automated damage detection methods have application to instrumented structures that are susceptible to types of damage that are difficult or costly to detect. The presented method has application to the detection of brittle fracture of welded beam-column connections in steel moment-resisting frames (MRFs), where locations of potential structural damage are known *a priori*. The method makes use of a prerecorded catalog of impulse response function (IRF) templates and a cross-correlation method to detect the occurrence, location, and time of structural damage in an instrumented building. The method is designed to recognize elastic waves radiated by the original brittle fracture event, where the event is not known to have occurred with certainty and the resulting damage may not be visible. An experimental study is conducted to provide insight into applying the method to a real structure. A series of hammer blows and bolt fractures is used to excite a small-scale steel frame to test whether cross-correlation techniques and catalogued IRF templates can be used to identify the occurrence and location of an assumed-unknown event. To investigate this method for a full-scale structure *in situ*, IRFs are experimentally obtained from a densely-instrumented

steel moment-resisting frame building. The recorded IRFs are easily observed over the ambient noise of the building. Results support the idea of using a nondestructive force to localize damage using high-frequency seismograms, though the method might be prone to false negatives (i.e., missed detections) when used to detect the presence of damage.

2.1 Introduction

Acoustic damage detection methods rely on the comparison of a recent signal to an archived baseline response function, known as a template. The template is recorded at a time when the structure is undamaged. The sensor network has a sampling rate that is high enough to capture the propagation of waves throughout the structure. Acoustic techniques have been explored experimentally and numerically for thin plates and beams, which serve as waveguides that effectively carry information from the location of structural damage to a receiver (Giurgiutiu and Cuc, 2005; Park et al., 2007; Wang et al., 2004; Wang and Rose, 2003). This information, namely differences in waveform and amplitude between the current signal and the template, is used to diagnose damage. Acoustic methods can be passive or active, and sensor networks can be permanently installed or temporary. Existing methods include pitch-catch, pulse-echo, time-reversal, and migration. In this paper, a complementary acoustic method is presented that makes use of a prerecorded catalog of IRFs and a cross-correlation method to passively detect the original failure event. This technique is different from existing acoustic methods as it is designed to use the elastic waves radiated by the original brittle failure event to both identify and localize damage. It is similar to the matched filter method, which has been successfully used in other fields to detect repeating small-magnitude earthquakes in noisy data (Anstey, 1964; Gibbons and Ringdal, 2006). The method has yet to be explored in the context of acoustic damage detection of civil structures.

2.2 Description of Proposed Damage Detection Method

The proposed method makes use of a prerecorded catalog of IRFs for an instrumented building to detect structural damage during a later seismic event. Continuous data collected on a passive network are screened for the presence of waveform similarity to one of the IRF templates. The method is outlined below.

1. Identify probable points of failure in an instrumented building before structural damage has occurred. As pre-Northridge steel MRFs are susceptible to the brittle failure of welded beam-column connections, these would be the locations of probable failure for this type of building.
2. At each labeled location, apply a short-duration high-frequency pulse (e.g. using a force transducer hammer). The response of the building at each instrument site is the IRF specific to that source location-receiver pair. The IRFs are archived in the catalog of templates to be used later to screen the high-frequency seismogram for a damage signal.
3. Screen data recorded at a later time for the presence of a damage event using the prerecorded templates. For each possible source location k , perform a running cross-correlation between the IRF templates for that source location and a moving window of the seismogram that recorded the shaking event, stacking over the receivers. Cross-correlation between the k^{th} IRF template g_i^k recorded by the i^{th} receiver and the seismogram x_i recorded by the i^{th} receiver is given by:

$$C_i^k(t) = \frac{\int_0^T g_i^k(\tau)x_i(t + \tau)d\tau}{\left(\int_0^T (g_i^k(\tau))^2d\tau \int_0^T (x_i(t + \tau))^2d\tau\right)^{1/2}}. \quad (2.1)$$

Time T is the duration of the template, and the cross-correlation is normalized by the autocorrelation values for the given time window. Compute the stacked cross-

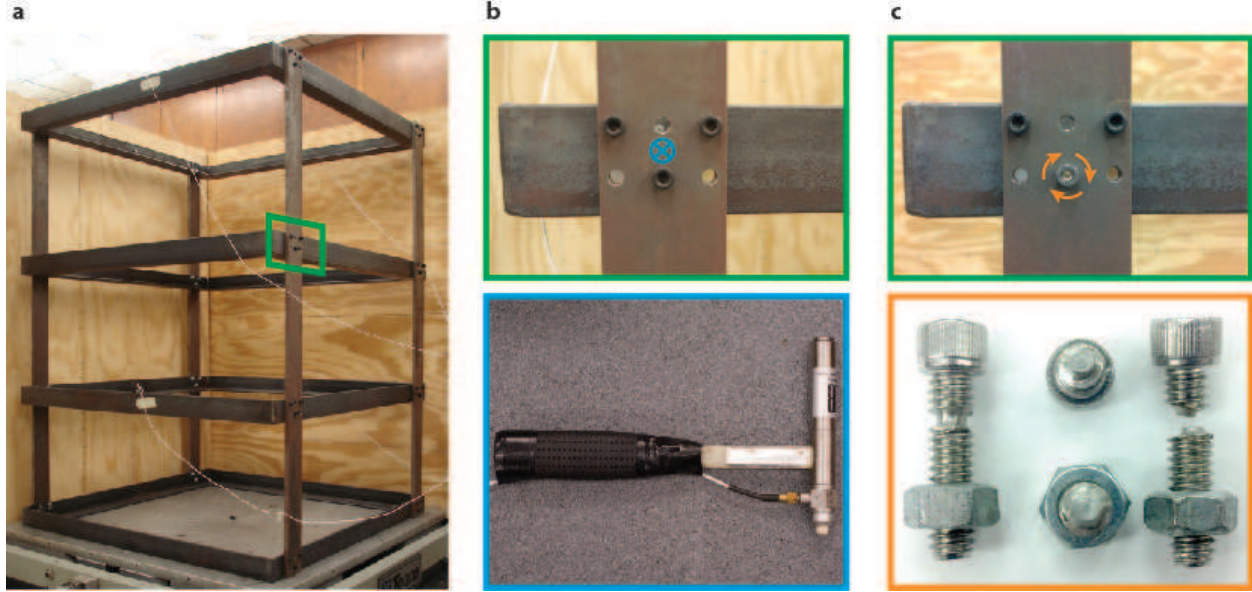


Figure 2.1: **Steel Frame: Experimental Setup.** **a**, The steel frame consists of three floors above ground and one floor at its base that is attached to a stationary shake table. The connections are moment-resisting, with three bolts firmly connecting the beams to columns. **b**, A force-transducer hammer is used to apply an impulsive force to a beam-column connection at the mark shown in blue, along an axis that points into the page. **c**, Bolt fracture is introduced by first substituting a bolt with a notch machined into it into a connection at the indicated location in orange. The bolt is torqued until it fractures.

correlation function by summing over the R receiver locations:

$$C^k(t) = \frac{1}{R} \sum_{i=1}^R C_i^k(t). \quad (2.2)$$

4. If damage occurred at or near the k^{th} source location, the stacked cross-correlation function given by Equation 2.2 should peak at a value close to unity at the correct time of the structural damage event. In the case of multiple locations of damage, then the stacked cross-correlation functions should each peak at a value close to unity at the corresponding times, provided the correct IRF templates are used. This procedure could be extended to the three-dimensional or discrete case.

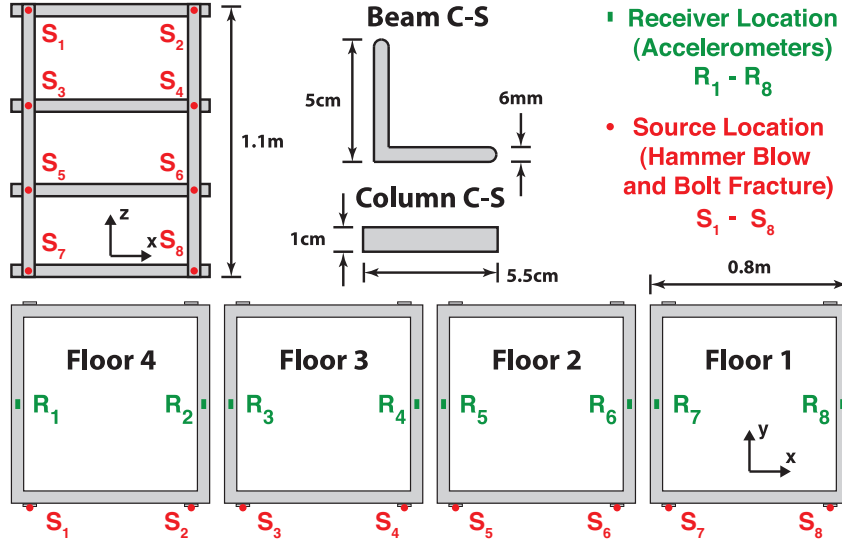


Figure 2.2: **Steel Frame: Receiver Locations.** The steel frame is instrumented with eight accelerometers in a layout that is similar to an instrumentation layout one might expect to find in the vibration monitoring of an actual building. The receivers record acceleration along the y-axis.

2.3 Experimental Study: Small-Scale Steel Frame

To study the feasibility of the proposed method, experimental tests were conducted on the small-scale steel frame shown in Figure 2.1. Three different configurations of damage state and source mechanism were tested: impulsive hammer blow applied to the undamaged frame, bolt fracture, and impulsive hammer blow applied to a frame with a damaged beam-column connection. The similarities and differences between the three cases were analyzed using waveform cross-correlation normalized by the autocorrelation value and stacked over the eight receiver locations. Results were averaged over the total number of trials.

2.3.1 Experimental Setup

A small-scale steel frame instrumented with eight uniaxial (y-axis) accelerometers, shown in Figure 2.1, was subjected to hammer blows and bolt fracture at beam-column connections. A sample frequency of 100 kHz and record duration of 2 seconds were used. The experimental setup included the following equipment (the corresponding specification sheets can be found in the Appendix A):

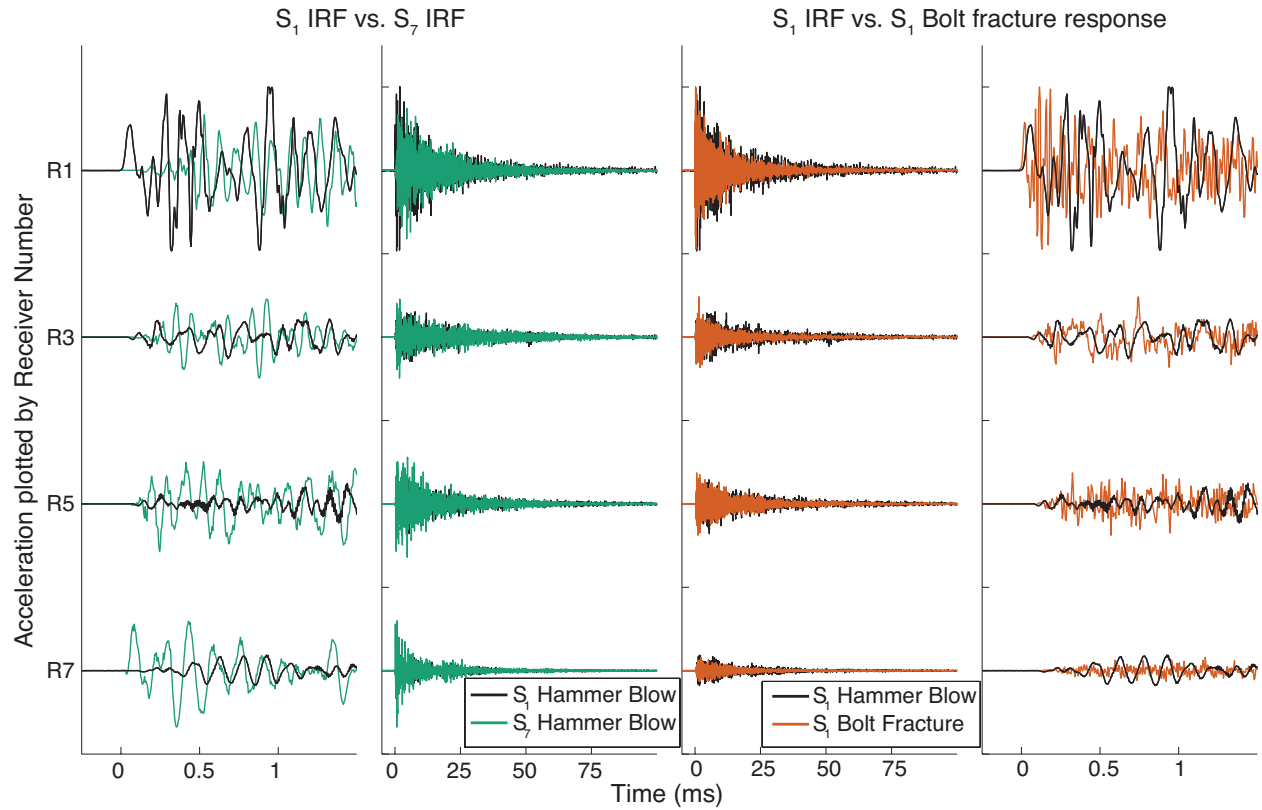


Figure 2.3: **Steel Frame: Example Accelerations.** A comparison of the IRFs for two hammer blows that were applied at different locations (S_1 and S_7) for the undamaged frame is shown on the left. A comparison of a prerecorded IRF with the response of the frame to bolt fracture at the same location (S_1) is plotted on the right. As can be seen from the comparison of IRFs, the arrival times and the relative amplitudes differ significantly between the two records, with the highest amplitudes and first arrivals occurring at the receiver location closest to the source location. As can be seen from the comparison of IRF with the response to colocated damage, the arrival times and the relative amplitudes are similar.

- Small-scale steel frame with a pinned base and bolted beam-column connections.
- High-sensitivity low-mass accelerometers and power supply.
- Force transducer hammer and power supply.
- USB multifunction data acquisition device.
- Laptop for data logging.

2.3.2 Experimental Results and Discussion

IRFs were generated by using a force transducer hammer to apply an impulsive force load along the y-axis to each of the eight beam-column connections (S_1 - S_8) shown in Figures 2.1 and 2.2. IRFs were obtained by exciting the frame using a hammer blow and recording the resulting acceleration. Seven trials were repeated at each source location. In order to determine whether these prerecorded IRFs could be used as an approximation to the frames response to structural damage (i.e., a fracture event) at the same source location, bolt fracture was also used to excite the structure in response to a damage event. A notched stainless steel socket cap screw was introduced into a beam-column connection. The screw replaced the bottom bolt shown in Figure 2.1. It was then loaded by torque tightening to the point of failure, and the response of the frame to the fracture was recorded on the eight accelerometers. Three trials were repeated at each of the four source locations S_1 , S_3 , S_5 , and S_7 . Finally, a tap test was conducted using the damaged frame; damage was introduced to the frame at a connection by removing all three bolts. These damage IRFs were compared with the pre-recorded IRFs.

As can be seen from the example acceleration time series shown in Figure 2.3, the response of the frame to bolt fracture consists of more high-frequency energy than does the IRF. The relative amplitudes and arrival times of the two responses are observed to be similar when the source is generated at the same location. The relative amplitudes are shown in Figure 2.4. Both the amplitudes and arrival times of the responses could be used for damage localization. The arrival times and amplitudes between IRFs generated by hammer blows applied at different source locations differ significantly.

The maximum amplitude of the stacked cross-correlation record is used as an indicator of how similar two responses are. Cross-correlations were first calculated at each receiver location, using the recorded pair of acceleration time series and autocorrelation normalization, as in Equation 2.1. The cross-correlations were then stacked over all eight receivers, as in Equation 2.2. Example cross-correlations are presented in Figure 2.5, where the cross-correlations of the IRFs generated by an impulsive hammer blow applied at location S_1 is

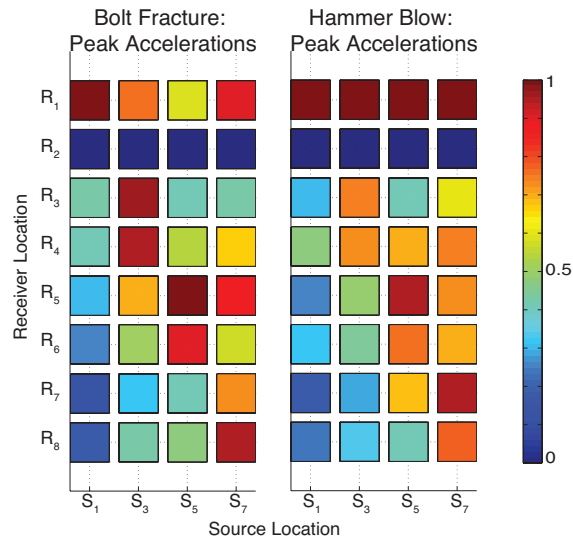


Figure 2.4: **Steel Frame: Comparison of Peak Accelerations in Response to Bolt Fracture and IRFs.** **a**, The peak acceleration is calculated for a given trial by taking the maximum absolute value of each of the eight acceleration records (at locations R_1 - R_8); the eight recorded peak accelerations are then normalized to range between zero and one for each trial. Peak accelerations are averaged over the number of trials and shown above. A total of three trials were conducted at each of the four source locations (S_1 , S_3 , S_5 , S_7). **b**, Similarly, the peak accelerations are computed for the IRFs applied at the same source locations. Again, a total of five trials is averaged for each of the four source locations (S_1 , S_3 , S_5 , S_7). There is general agreement of peak accelerations between the response to the two colocated different source mechanisms. The data recorded at location R_2 were corrupted, and were thus omitted.

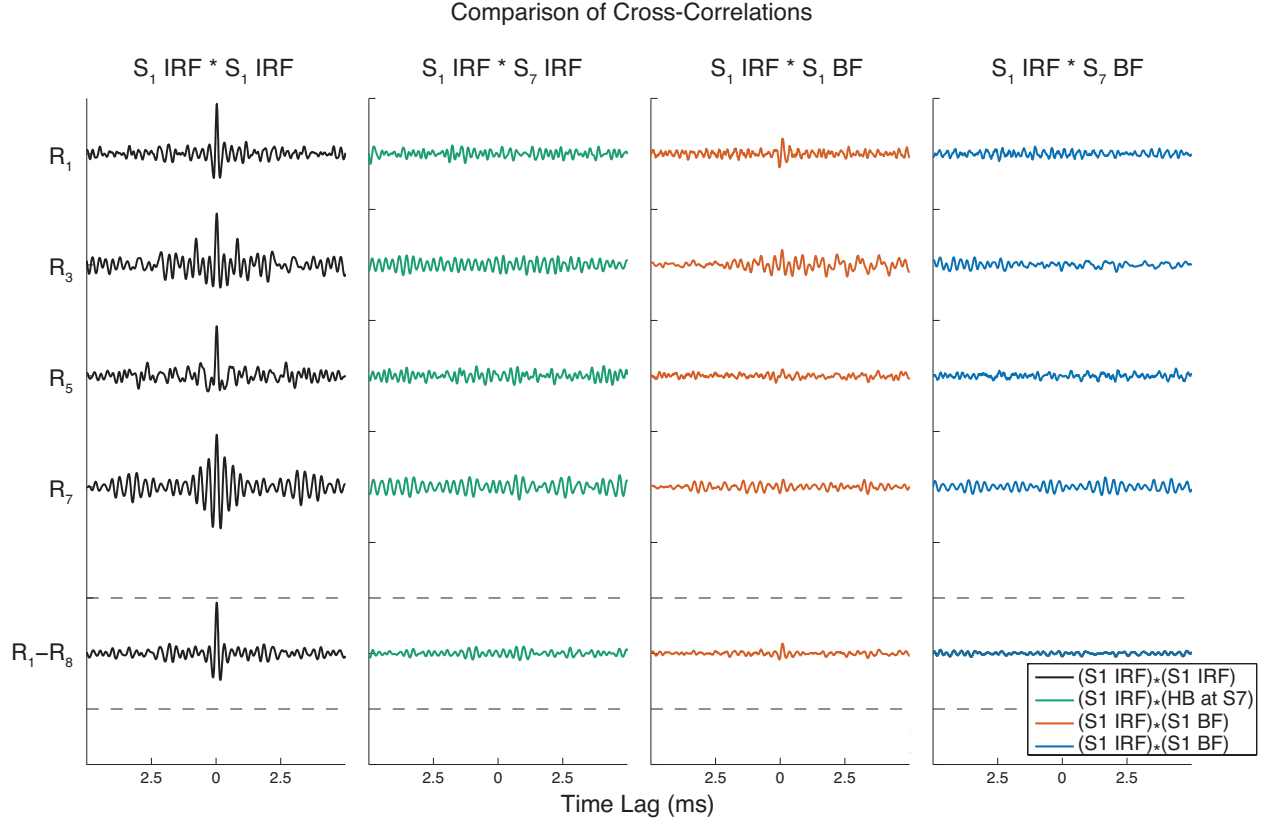


Figure 2.5: **Steel Frame: Example Cross-Correlations.** Example cross-correlations are shown using the impulse response function generated by a hammer blow applied at S_1 with (left) a second impulse response function generated by a hammer blow applied at S_1 , (left-middle) the impulse response function generated by a hammer blow applied at S_7 , (right-middle) the response of the frame to bolt fracture at location S_1 , and (right) the response of the frame to bolt fracture at location S_7 . The stacked cross-correlations are plotted on the bottom, with dashed black lines referencing values of 1 and -1. The maximum value of the stacked cross-correlation for each of the four illustrated cases is 0.91, 0.13, 0.18, and 0.07, respectively. Normalized waveform cross-correlations are performed using the entire acceleration time series.

cross-correlated with the following records: 1) a second IRF generated by a hammer blow applied at S_1 , 2) an IRF generated by a hammer blow applied at S_7 , 3) the response of the frame to bolt fracture at S_1 , and 4) the response of the frame to bolt fracture at S_7 . The maximum value of the stacked cross-correlation for each of the four illustrated cases is 0.91, 0.13, 0.18, and 0.07, respectively.

To determine the degree of similarity between the IRFs, the cross-correlation of every possible pair was computed and is presented in Table 2.1. The pair of IRFs have a cross-correlation value near to one when their sources are colocated and a value close to zero when

their sources are applied at different locations. The time delay from the cross-correlation is compared to the relative time difference of the hammer blows in Table 2.1, and a high level of precision is observed in determining the moment at which the hammer blow was applied, typically to within 10 μ s.

Cross-correlations were also computed between the prerecorded IRFs and the frame's response to bolt fracture. This was done in order to determine the degree of similarity between the two responses. Specifically, the frame's prerecorded IRFs were cross-correlated with the response of the frame to bolt fracture. Each possible pair of bolt failure source location and IRF source location was considered, and the correlation values are presented in Table 2.3. The response of the frame to bolt fracture correlates best with the response of the frame to the colocated hammer blow. However, these correlation values are not close to unity; they range from 0.17 to 0.19. This experimental analysis suggests that the method may not be very robust in the case of damage detection.

Correlation values were improved by weighting the individual cross-correlation records proportionally to the amplitude of the response to bolt failure at each recorded location prior to stacking them. The maximum value of the amplitude of the stacked cross-correlation was determined, and these values are tabulated in Table 2.4. The correlation values along the diagonal range from 0.2 to 0.45. The modified Equation 2.2 is:

$$C^k(t) = \frac{\sum_{i=1}^R \max|x_i|C_i^k(t)}{R \left(\sum_{i=1}^R \max|x_i|^2 \right)^{1/2}}. \quad (2.3)$$

If the envelopes are used instead of the waveforms for cross-correlation, then the terms along the diagonal are close to unity, but so are the off-diagonal terms, albeit only slightly smaller than the diagonal values. This form of cross-correlation would be feasible in the cases with accelerations that have larger differences in arrival times and shorter length of pulses. Other signal processing techniques that were applied in various combinations were not found to significantly improve the correlation values, and they include:

- Filtering - high-pass or low-pass.

- Polarity/phase - using the analytic signal, envelope, or amplitude.
- Shortening the length of the template and adjusting the normalization scheme accordingly.
- Integrating or differentiating the record.
- Recording the maximum value of the amplitude of the stacked cross-correlation.
- Cross-correlating with the IRFs recorded on the damaged frame.
- Creating a template using two IRFs applied in opposite directions.

Correlation values calculated using the responses to bolt fracture, found in Table 2.7, can serve as a rough upper bound estimate for the maximum correlation values one might expect to obtain by using waveform cross-correlation of an IRF with the response to bolt fracture. The correlation values for the response of the frame to colocated bolt fracture range from 0.7 to 0.87. These values demonstrate the surprisingly high level of consistency between the response of the frame to bolt fracture between different trials. This also indicates that, in the case where the damage signal is generated by a repeating source, the initially-detected signal can be used to as a template to detect the next occurrence of the damage signal in the time series.

Finally, IRFs for a damaged frame were obtained by performing a tap test on the frame with a damaged beam-column connection. Damage was introduced by removing all three bolts from a connection (S_1 , S_3 , S_5 , or S_7), with the stiffness of the frame rigidly holding the beam and column in place. An impulsive hammer blow was applied to each of the eight source locations, for each of the four damaged connection cases. This was performed a total of three times. To highlight differences in structural response before and after damage occurred, the prerecorded IRFs were cross-correlated with the response of the damaged frame to an impulsive hammer blow applied at the same source location, for each of the four damaged connection cases. Results were averaged over 15 total trials and are presented in Table 2.6. There are significant differences between the response of the frame before

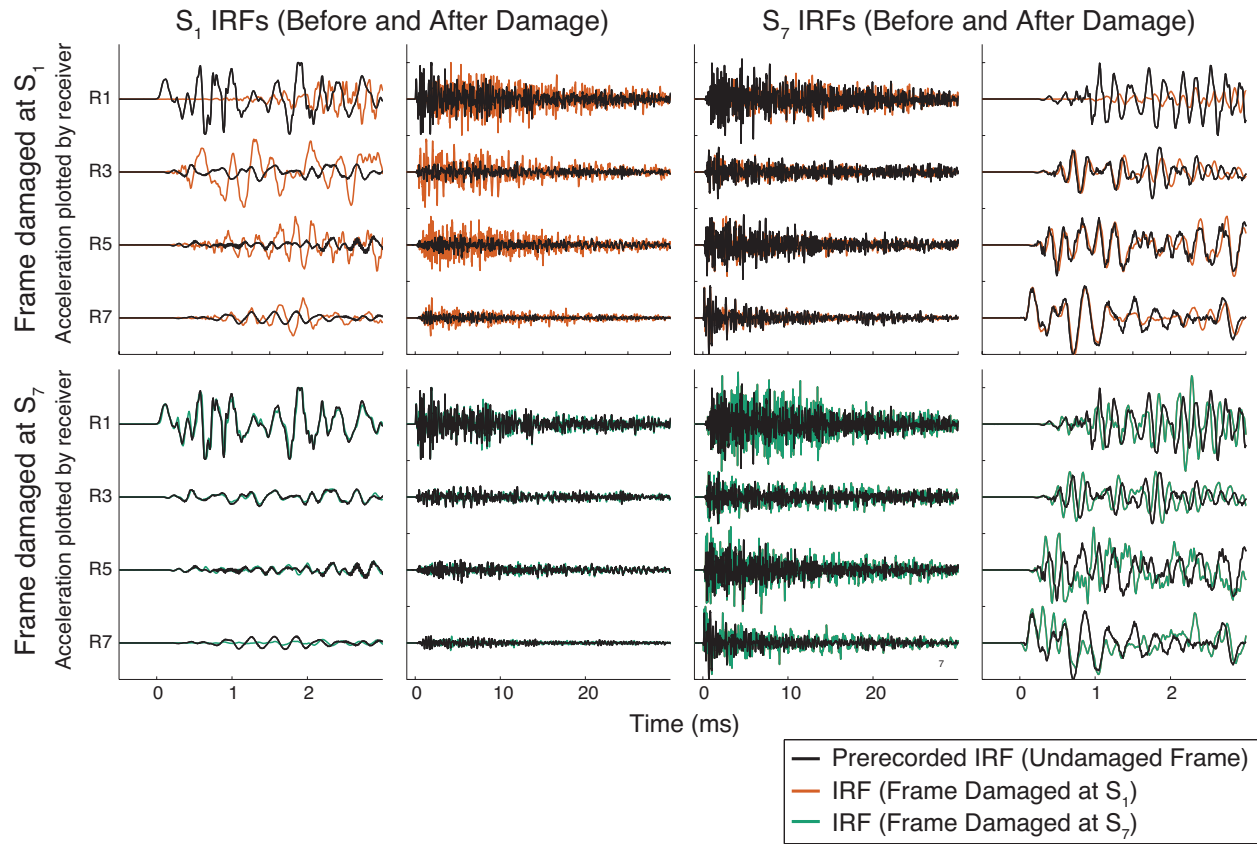


Figure 2.6: **Steel Frame: Comparison of IRFs Before and After Damage.** Prerecorded IRFs are compared with IRFs generated when the frame is in a damaged state. The first two columns plot accelerations generated by a hammer blow applied at location S_1 ; the second two columns plot accelerations generated from a hammer blow applied at location S_7 . The color of the signal indicates the damage state of the frame, with undamaged shown in black, damaged at S_1 shown in orange, and damaged at S_7 shown in green. As can be surmised from the plots in Columns 1 and 4, the initial pulse propagates through the medium undisturbed until it passes through the region of damage. At this point, the response of the damaged frame begins to diverge from the response of the undamaged frame. A high-frequency signal is generated when the hammer blow is applied at the damaged source location, resulting in larger accelerations on all floors. The relative amplitudes of acceleration have been preserved for each trial.

damage was introduced and the response of the frame after damage was introduced, with typical correlation values of 0.5. For comparison, these values range from 0.78-0.85 for the undamaged case. Furthermore, the observed correlation values along the diagonal are much lower than are the values of the off-diagonal terms, and they range from 0.11 to 0.41. This means that the IRF of the damaged frame is observed to differ the most from the pre-recorded IRF when the source is applied at the location of damage. As seen in Figure 2.6, the damaged connection is observed to act as a high-frequency source when the hammer blow is applied to the damaged connection. The high-frequency signal is presumably generated by slight mechanical impact and slippage within the interface between the column and the beam. This relative motion is very small as the frame is very stiff and no motion is detected by visual observation. The fact that the lowest cross-correlation value occurs for damage introduced at the top of the column supports this hypothesis. The column is less stiff at the damaged location than it is in other cases, due to the free boundary at the top floor. The introduction of damage changes the boundary conditions at the damaged connection, as the screws of the undamaged connections tightly secure together the beam and column. The frame is rigid enough that even by removing the bolts from a particular connection, the beam and column are firmly held in place. When damage is introduced to a beam-column connection at one of the lower floors, the stiffness of the column near the damaged connection is relatively large as the column is bolted together with the floors immediately above and below the damaged connection. When damage is introduced to the top floor, the stiffness of the column is not as high, as it is only screwed together with the lower floor and has a free boundary at the top. Hence, it is more flexible and is able to experience larger motions at the beam-column interface. A visual comparison of the different correlation values can be found in Figure 2.7.

2.3.3 Blind Tap Test

A blind tap test was performed to confirm whether the pre-recorded IRFs could be used to determine where and when a later hammer blow occurred. A number of tap tests were

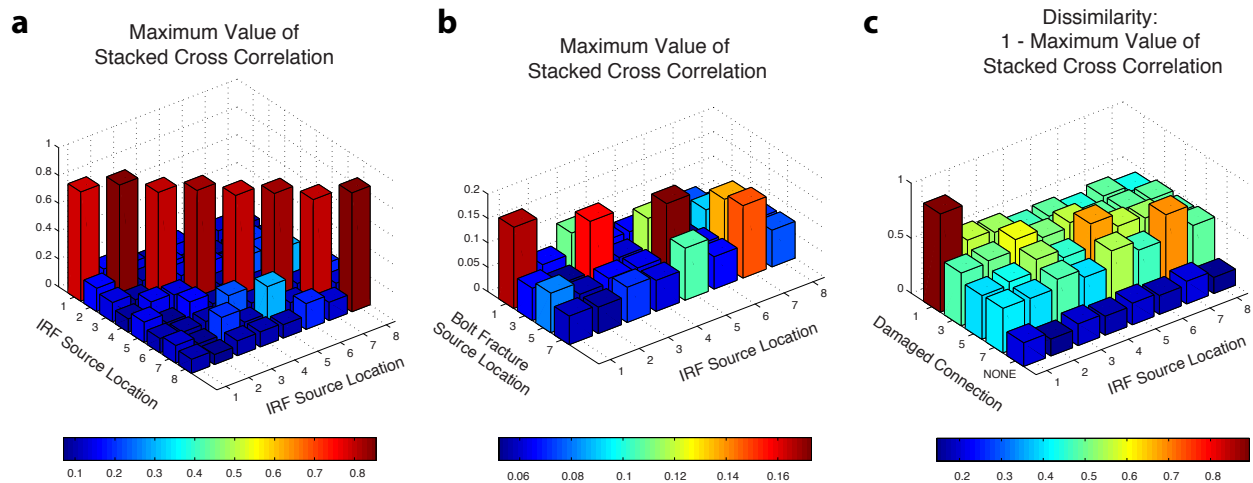


Figure 2.7: **Steel Frame: Comparison of Correlation Values Before, During, and After Damage.** **a**, The correlation values using the IRFs recorded before damage (see Table 2.1) are plotted. There is a high degree of similarity between pairs with colocated sources. **b**, The correlation values generated using the prerecorded IRFs and responses to bolt fracture are much smaller for the values generated using two colocated IRFs (see Table 2.3). Values along the diagonal range between 0.15 and 0.20. These values can be improved to 0.20 and 0.45 if, before stacking, the cross-correlations at a given receiver are scaled proportionally to the amplitude of the peak absolute acceleration recorded at that receiver in the response to bolt failure. **c**, The dissimilarity values (one minus the peak stacked correlation values) using the IRFs recorded before and after damage (see Table 2.6) are plotted. There is a high degree of dissimilarity between pairs with colocated sources, and especially when the source is applied at the damaged location.

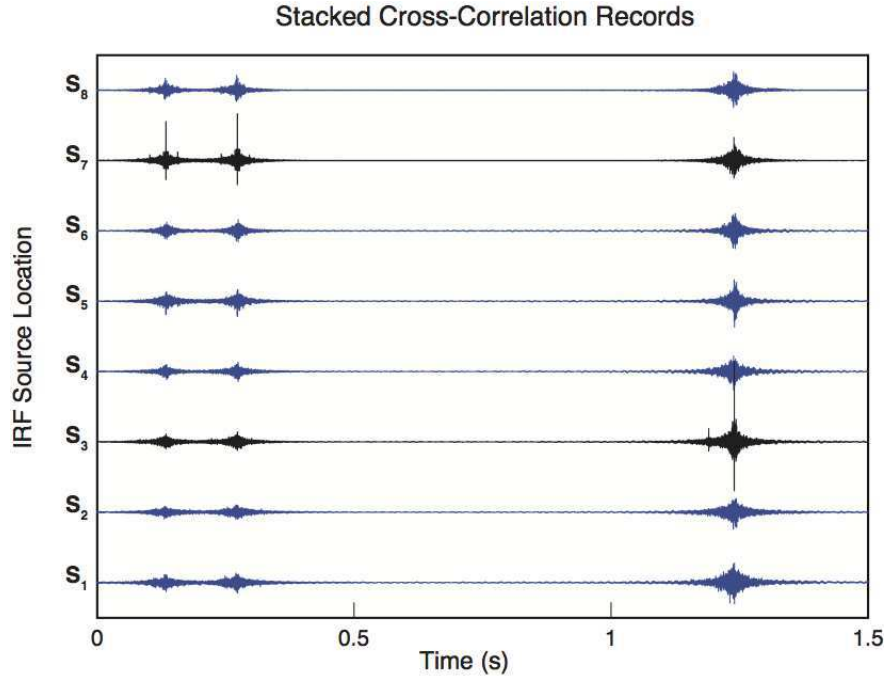


Figure 2.8: **Steel Frame: Blind Tap Test Using Hammer Blows.** A blind tap test is conducted using an acceleration time series containing the response of the frame to three hammer blows applied to unknown locations. A number of tap tests were performed, and one of the tests was selected at random and analyzed. The stacked cross-correlation values, computed using the test data and one of the IRFs, is used to determine where the hammer blow was applied. The actual locations were revealed only after the selection had been made. As can be determined from the stacked correlations shown above, the hammer blows were applied at locations S_7 , S_7 , and S_3 at times 0.15 s, 0.30 s, and 1.25 s, respectively.

performed, and one of the tests was selected at random and analyzed to see if the source locations could be correctly determined. The blind tap test, shown in Figure 2.8 below, was performed using three hammer blows applied in unknown locations. Stacked cross-correlations between the test data and each IRF (one for each source location) were computed and compared to determine the three locations. Three cross-correlation peaks stand out in the comparison: S_7 , S_7 , and S_3 . The actual locations were revealed after the selection had been made. The determined locations were indeed the three locations used for the blind test.

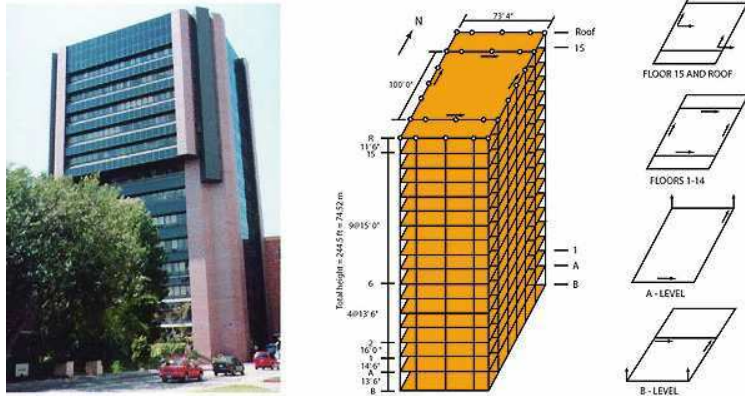


Figure 2.9: **Factor Building: Instrumentation.** A 16-story moment-resisting frame building located at UCLA, the Factor Building is densely instrumented with a 72-channel accelerometer network. Image courtesy of Kohler et al. (2009).

2.4 Experimental Study:

Steel Moment-Resisting Frame Building

A 16-story moment-resisting frame building located at UCLA, the Factor Building is densely instrumented with a 72-channel accelerometer network (see Figure 2.9). IRFs were experimentally obtained using a rubber mallet to excite the building at a few locations close to moment-resisting connections. Both 500 sps and 100 sps data was recorded. The IRFs were obtained by recording the acceleration response of the building to hammer blows applied at the following locations:

15th Floor NW: Two hammer blows were applied next to the northwest corner below a major moment-resisting connection.

15th Floor SW: Two hammer blows were applied next to the southeast corner, base of column, below major moment-resisting connection.

3rd Floor: One hammer blow was applied at the stairs.

Each of the five IRFs is clearly observable over the ambient response of the structure, at both 500 sps and downsampled to 100 sps. The IRF generated by applying a hammer blow at the northwest corner of the 15th floor, shown Figure 2.10, has a high signal-to-noise ratio

(SNR) for the acceleration records on the the 3rd floor through the 16th floor stations located on the west side of the building with a northward orientation. The SNR for this record is lower for acceleration records located on the other side of the building, as seen in Figure 2.11. Reasons for this include the distance to the source, and the effectiveness of the beams and columns in transmitting the high-frequency energy generated by the hammer blow to other regions of the building. While the column to which the hammer blow was applied may be efficient at transmitting the high-frequency energy to lower floors on the same side of the building, this does not indicate that the energy will travel well around corners or between structural members.

IRF templates, shown in Figure 2.11, are formed using the recorded accelerations at all floors within a short duration (0.2 seconds) after the hammer blow was applied. The largest amplitude acceleration and first arrival time occurs at the receiver located closest to the source location. To measure the degree of similarity between IRFs, correlation values are calculated. Waveform cross-correlation was performed using templates with a length of 0.2 seconds. Results were stacked and normalized, so that the resulting correlation values range between zero and one. Colocated IRFs have the highest correlation values close to 0.5. These values could be improved by only including signals with a high SNR in the IRF template rather than all existing records, and also by forming the IRF templates by stacking using a few trials conducted at each location. Although the 15 NW IRF and 15 SE IRF were generated by using hammer blows applied at the same floor, the IRFs differ significantly, with a maximum correlation value of 0.10. This means that it is possible to distinguish between locations within a single floor using this method.

2.5 Conclusion

An experimental study was conducted to provide insight into a damage detection method that makes use of a prerecorded catalog of IRF templates and a cross-correlation method to detect the occurrence and location of structural damage in an instrumented building. Impulsive hammer blows and bolt fracture were applied to a small-scale steel frame to test the

Impulse Response Function
for Hammer Blow Applied at Floor 15 (NW Corner)

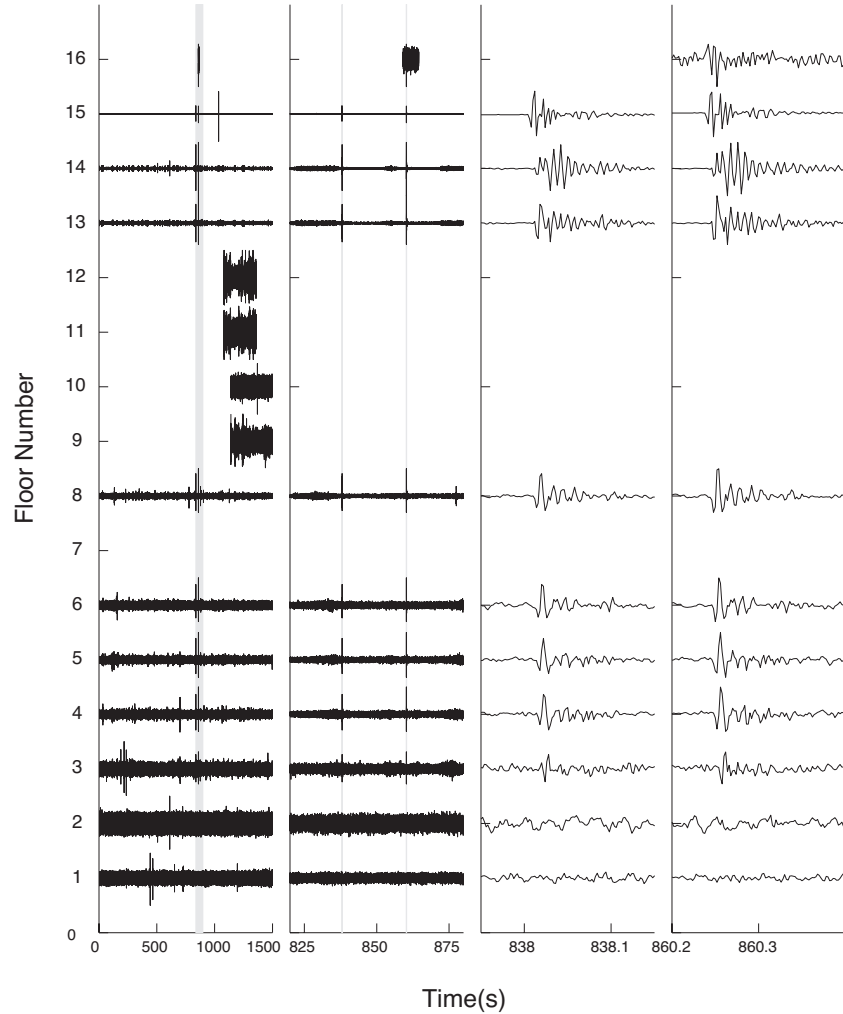


Figure 2.10: **Factor Building: Example IRF.** An IRF was generated using a rubber mallet to apply a hammer blow next to the northwest corner below a major moment-resisting connection. In the first column, 25 minutes of data are shown, with a minute-long segment shaded in gray. This minute-long segment is expanded in the second column, where the two IRFs, highlighted in gray, are clearly observable over the ambient response of the structure. The recorded IRFs of the structure to two hammer blows at this location are plotted for Floors 1-16 using the seismometers located at the west position with an orientation pointing north and recording at 500 sps. There is a high degree of consistency between the two trials, with high signal-to-noise ratios from the 3rd floor through the 16th floor. Each acceleration record was normalized to better view the waveform, and the relative amplitudes were not preserved. Some of the sensors were not recording at the time of testing, and those records are missing from the figure.

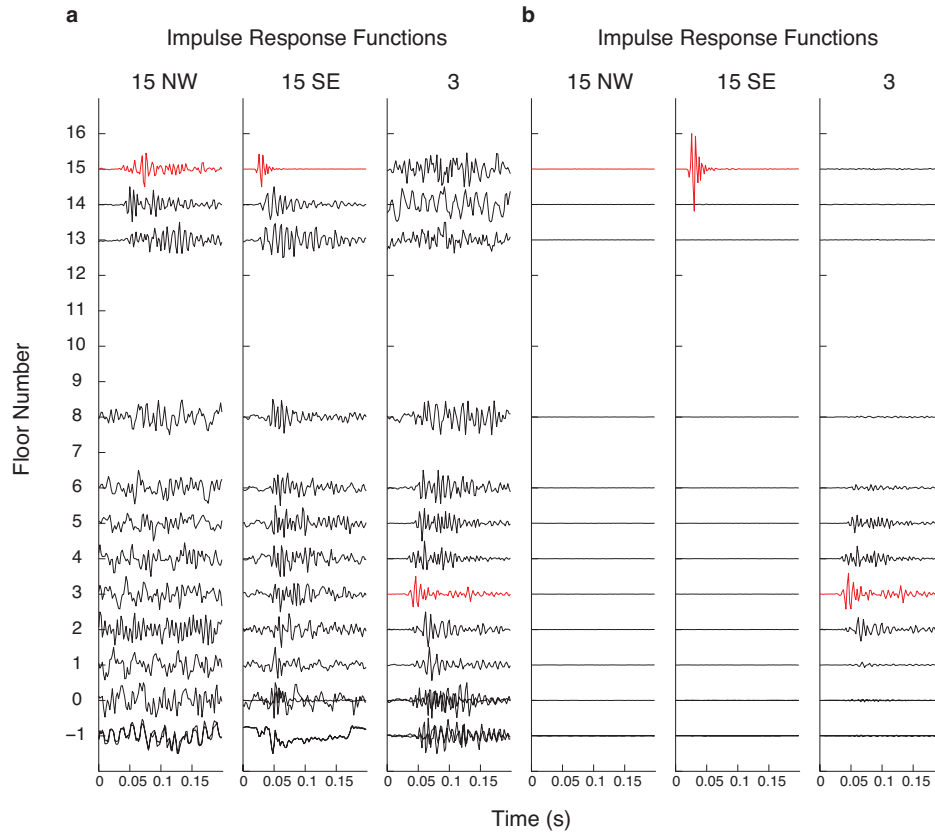


Figure 2.11: **Factor Building: Comparison of Impulse Response Functions.** Impulse response functions were experimentally obtained for a steel-moment-resisting frame building *in situ* by applying a hammer blow near to a moment-resisting-beam-column connection using a rubber mallet. Both 100 sps and 500 sps data were recorded, and the IRF is clearly visible in both cases; the 500 sps data is plotted above. A high signal-to-noise ratio (SNR) is obtained for stations located close to the hammer blow on the same side of the building. The stations shown above are located on the south side of the building and oriented eastward. The SNR could be improved by stacking the IRFs. There is a clear difference in arrival times and amplitudes between IRFs generated by hammer blows applied at different source locations. In **a**, each record has been normalized to better view the waveforms. In **b**, the set of acceleration records generated by a hammer blow have been normalized using the same value, so that the relative amplitudes have been preserved. The largest amplitudes are recorded on the closest seismometers to the hammer blow, on the same floor. The station on the same floor to which the hammer blow was applied is highlighted in red.

feasibility of applying the method to a building. The similarity between structure responses was evaluated using a cross-correlation method. The main findings of this chapter are:

1. IRFs were successfully obtained for an existing steel moment-resisting-frame building *in situ*. Not only were the IRFs clearly observable over ambient noise, the waveforms were also very consistent between trials with colocated sources, with correlation values typically greater than 0.8. For IRFs generated by hammer blows at different locations, significant differences were observed in arrival times, peak accelerations, and waveforms using eight accelerometers recording at 100 kHz. The data supports the idea of using hammer blow data to localize damage to a single column within a story. A sampling rate of 100 sps, though preferably 500 sps, seems to be high enough to capture the IRFs in the Factor building.
2. The application of the proposed damage detection method to the small-scale frame suggests that the IRF is not a robust approximation of the response to bolt failure. The method may also be suitable for damage localization, especially if it is combined with information about the arrival times and peak accelerations. While the IRFs cross-correlated well with each other and the responses to bolt fracture cross-correlated well with each other when the sources were colocated, the IRFs and responses to bolt fracture did not. However, in all considered cases, the IRF that had the highest correlation value with the response of the frame to bolt failure was the colocated IRF. Improvements in the correlation values were made by using an amplitude-dependent normalization that scaled with the maximum amplitude of acceleration at each receiver in response to bolt fracture. Information, such as arrival times and peak accelerations, can also be indicators of where damage occurred; this is of significance for sparsely-instrumented structures.
3. The response of the frame to bolt fracture was observed to be surprisingly consistent between trials (correlation values of 0.70-0.85 for responses with colocated sources). This suggests that the mechanism that occurs at the moment of bolt failure is consistent between trials, and a hammer blow does not well-characterize this source. This also

implicates that if a building were to undergo damage that resulted in the creation of a repeating source, a repeating high-frequency, short-duration signal might be observed in the acceleration time series. This could be generated by damage cases such as in the case of a breathing crack that repeatedly opens and closes, or a change in boundary conditions that increases the flexibility of a member and allows for the excitation of traveling waves.

4. The pre-recorded IRFs differed significantly from the IRFs that were recorded when the frame was in a damaged state, with typical cross-correlation values of 0.5, as compared to pre-damage values of 0.8. By comparing the generation of waves propagating through the frame, it was seen that the response of the damaged structure to a hammer blow applied at a given location begins to diverge from the response of the undamaged structure only after the elastic waves recorded at a given receiver location passed through the region of damage. This phenomenon is similar to the guided wave methods used in acoustic damage detection methods, and it also has potential to be used for damage detection in larger-scale structures. It would be necessary to use a repeatable mechanism to excite the structure over time, preferably under similar environmental conditions, and differences between the baseline signal and the subsequent recorded signal would be used to indicate damage. Damage might be located through an inverse problem approach that makes use of a finite-element model.
5. The application of a hammer blow to a damaged connection resulted in a low correlation value with the pre-recorded IRF generated by a colocated hammer blow. In this case, the damaged connection was observed to also act as a high-frequency source, most likely due to motion generated at the interface of the beam and column. Applying a hammer blow to a cracked beam or column in a real building may or may not result in high-frequency energy generated at the crack interface. Presumably, if a beam has a crack and the two sides of the crack are not held firmly together, e.g., a vertical crack in a beam, a hammer blow applied in the vicinity of the crack could result in mechanical slippage and impact caused by the relative motion at the crack interface. If, on the

other hand, the crack is firmly held closed, as might be the case for a horizontal crack in a column, high-frequency energy might not be generated at the crack interface in response to a nearby hammer blow.

6. As the responses to bolt fracture correlated just as well with pre-recorded IRFs as they did with the post-damage IRFs, it may be desirable to record the IRFs after an earthquake has occurred, when the building is in a potentially damaged state. In this way, there is an additional chance of detecting any high-frequency energy that is generated within a cracked interface at a damaged connection. (Also, if the building is never subjected to a large earthquake, there will be no need to conduct the hammer blow trials in the first place.) One advantage of having previously-recorded IRFs, however, is that they can be directly compared with post-earthquake IRFs, in order to detect damage in the frame by differences between them.

		IRF: Hammer Blow Source Location								
		S_1	S_2	S_3	S_4	S_5	S_6	S_7	S_8	
IRF: Hammer Blow Source Location	S_1	μ	0.85	0.22	0.12	0.10	0.12	0.09	0.09	0.10
		σ	0.06	0.01	0.02	0.01	0.01	0.01	0.01	0.01
		N	21	49	49	49	49	49	49	49
	S_2	μ	0.22	0.83	0.10	0.12	0.10	0.10	0.10	0.09
		σ	0.01	0.06	0.01	0.03	0.01	0.01	0.01	0.01
		N	49	21	49	49	49	49	49	49
	S_3	μ	0.12	0.10	0.86	0.12	0.19	0.12	0.19	0.12
		σ	0.02	0.01	0.05	0.01	0.01	0.01	0.01	0.01
		N	49	49	21	49	49	49	49	49
	S_4	μ	0.10	0.12	0.12	0.83	0.09	0.18	0.11	0.15
		σ	0.01	0.03	0.01	0.05	0.01	0.02	0.01	0.02
		N	49	49	49	21	49	49	49	49
	S_5	μ	0.12	0.10	0.19	0.09	0.82	0.11	0.17	0.14
		σ	0.01	0.01	0.01	0.01	0.05	0.01	0.03	0.01
		N	49	49	49	49	21	49	49	49
	S_6	μ	0.09	0.10	0.12	0.18	0.11	0.78	0.13	0.16
		σ	0.01	0.01	0.01	0.02	0.01	0.06	0.01	0.04
		N	49	49	49	49	49	21	49	49
	S_7	μ	0.09	0.10	0.19	0.11	0.17	0.13	0.80	0.18
		σ	0.01	0.01	0.01	0.01	0.03	0.01	0.06	0.02
		N	49	49	49	49	49	49	21	49
	S_8	μ	0.10	0.09	0.12	0.15	0.14	0.16	0.18	0.80
		σ	0.01	0.01	0.01	0.02	0.01	0.04	0.02	0.04
		N	49	49	49	49	49	49	49	21

Table 2.1: **Steel Frame: Correlation Values (Undamaged Frame IRFs)**. IRFs were generated by using a force transducer hammer to apply an impulsive force load along the y-axis to each of the eight beam-column connections (S_1 - S_8). The correlation values are close to unity when the IRFs are colocated. A total of seven hammer blows were delivered at each source location. Cross-correlations were first calculated at each receiver location, using the two different records and autocorrelation normalization. The cross-correlations were then stacked over all eight receivers. The maximum amplitude of the stacked cross-correlation is recorded, averaged over the total number of pairs (21 total for pairs consisting of two identical source locations and 49 total for pairs consisting of two distinct source locations), and presented above. Waveform cross-correlation was performed using the entire record. Values calculated using responses with colocated sources are highlighted in bold.

		IRF: Hammer Blow Source Location								
		S_1	S_2	S_3	S_4	S_5	S_6	S_7	S_8	
IRF: Hammer Blow Source Location	S_1	μ_t	-7	1370	-1900	2500	-620	-840	2600	470
		σ_t	15	15	2300	930	840	2700	5900	2200
		N	21	49	49	49	49	49	49	49
	S_2	μ_t	1370	5	-2100	2500	-2100	-1600	-2100	900
		σ_t	15	17	1800	3900	2400	5400	1600	5800
		N	49	21	49	49	49	49	49	49
	S_3	μ_t	-1900	-2100	-20	-1200	190	-40	600	-2000
		σ_t	2300	1800	33	2000	250	2100	30	1900
		N	49	49	21	49	49	49	49	49
	S_4	μ_t	2500	2500	-1200	14	-140	330	-830	420
		σ_t	930	3900	2000	24	2700	27	2000	58
		N	49	49	49	21	49	49	49	49
	S_5	μ_t	-620	-2100	190	-140	4	950	280	-2300
		σ_t	840	2400	250	2700	23	2700	69	1100
		N	49	49	49	49	21	49	49	49
	S_6	μ_t	-840	-1600	-40	330	950	-3	1300	520
		σ_t	2700	5400	2100	27	2700	25	890	760
		N	49	49	49	49	49	21	49	49
	S_7	μ_t	2600	-2100	600	-830	280	1300	-1	1400
		σ_t	5900	1600	30	2000	69	890	23	332
		N	49	49	49	49	49	49	21	49
	S_8	μ_t	470	900	-2000	420	-2300	520	1400	7
		σ_t	2200	5800	1900	58	1100	760	332	12
		N	49	49	49	49	49	49	49	21

Table 2.2: **Steel Frame: Time Errors in Correlations (Undamaged Frame IRFs)**. The accompanying time error (in units μs) from the previous table’s cross-correlation values are presented above. The time error is computed as the difference between the time lag of the stacked cross-correlation and the difference in times at which the force was applied, as measured by the force transducer hammer. A very small time error, typically less than 10 μs , is observed. Values calculated using responses with colocated sources are highlighted in bold.

		IRF: Hammer Blow Source Location								
		S_1	S_2	S_3	S_4	S_5	S_6	S_7	S_8	
Bolt Fracture Source Location	S_1	μ	0.19	0.08	0.13	0.08	0.08	0.07	0.09	0.06
		σ	0.05	0.09	0.01	0.01	0.07	0.01	0.01	0.01
		N	15	15	15	15	15	15	15	15
	S_3	μ	0.08	0.06	0.18	0.07	0.14	0.06	0.10	0.06
		σ	0.01	0.01	0.02	0.01	0.01	0.01	0.01	0.01
		N	15	15	15	15	15	15	15	15
	S_5	μ	0.09	0.07	0.08	0.07	0.19	0.07	0.16	0.08
		σ	0.01	0.00	0.01	0.01	0.03	0.01	0.02	0.01
		N	15	15	15	15	15	15	15	15
	S_7	μ	0.07	0.06	0.08	0.07	0.13	0.08	0.17	0.08
		σ	0.01	0.00	0.01	0.01	0.03	0.01	0.03	0.01
		N	15	15	15	15	15	15	15	15

Table 2.3: **Steel Frame: Correlation Values (IRFs and Response to Bolt Fracture)**. IRFs were generated by using a force transducer hammer to apply an impulsive force load along the y-axis to each of the eight beam-column connections (S_1 - S_8). A total of five hammer blows were delivered at each source location. Damage was introduced through bolt fracture at one of the connections (S_1, S_3, S_5, S_7). Three trials were repeated for each source location. Cross-correlations were first calculated at each receiver location, using the two different records and autocorrelation normalization. The cross-correlations were then stacked over all eight receivers. The maximum amplitude of the stacked cross-correlation is recorded, averaged over the total number of pairs. Waveform cross-correlation was performed using the entire record. Values calculated using responses with colocated sources are highlighted in bold.

		IRF: Hammer Blow Source Location								
		S_1	S_2	S_3	S_4	S_5	S_6	S_7	S_8	
Bolt Fracture Source Location	S_1	μ	0.45	0.18	0.35	0.17	0.20	0.16	0.23	0.16
		σ	0.07	0.03	0.02	0.02	0.03	0.02	0.03	0.01
		N	15	15	15	15	15	15	15	15
	S_3	μ	0.13	0.11	0.30	0.11	0.22	0.10	0.17	0.10
		σ	0.02	0.02	0.05	0.02	0.03	0.02	0.02	0.01
		N	15	15	15	15	15	15	15	15
	S_5	μ	0.11	0.08	0.08	0.09	0.25	0.10	0.25	0.10
		σ	0.02	0.01	0.02	0.02	0.06	0.02	0.05	0.02
		N	15	15	15	15	15	15	15	15
S_7	μ	0.05	0.05	0.07	0.06	0.09	0.06	0.20	0.09	
	σ	0.01	0.01	0.02	0.01	0.03	0.01	0.06	0.02	
	N	15	15	15	15	15	15	15	15	

Table 2.4: **Steel Frame: Correlation Values Using Peak Acceleration Normalization (IRFs and Response to Bolt Fracture)**. IRFs were generated by using a force transducer hammer to apply an impulsive force load along the y-axis to each of the eight beam-column connections (S_1 - S_8). A total of five hammer blows were delivered at each source location. Damage was introduced through bolt fracture at one of the connections (S_1, S_3, S_5, S_7). Three trials were repeated for each source location. Cross-correlations were first calculated at each receiver location, using the two different records and autocorrelation normalization. The cross-correlation computed using the records at a given receiver was further scaled by the peak amplitude of the acceleration recorded at that receiver, given by Equation 2.3. The maximum amplitude of the stacked cross-correlation is recorded, averaged over the total number of pairs, and divided by the square root of the sum of the squared peak amplitudes. Waveform cross-correlation was performed using the entire record. Values calculated using responses with colocated sources are highlighted in bold.

		Bolt Fracture Source Location				
		S_1	S_3	S_5	S_7	
Bolt Fracture Source Location	S_1	μ	0.70	0.10	0.08	0.09
		σ	0.02	0.01	0.01	0.01
		N	3	9	9	9
	S_3	μ	0.10	0.83	0.08	0.08
		σ	0.01	0.06	0.01	0.01
		N	9	3	9	9
	S_5	μ	0.08	0.08	0.87	0.11
		σ	0.01	0.01	0.03	0.01
		N	9	9	3	9
	S_7	μ	0.09	0.08	0.11	0.85
		σ	0.01	0.01	0.01	0.05
		N	9	9	9	3

Table 2.5: **Steel Frame: Correlation Values (Response to Bolt Fracture)**. Damage was introduced through bolt fracture at one of the connections (S_1, S_3, S_5, S_7). Three trials were repeated for each source location. Cross-correlations were first calculated at each receiver location, using the two different records and autocorrelation normalization. The cross-correlations were then stacked over all eight receivers. The maximum amplitude of the stacked cross-correlation is recorded, averaged over the total number of pairs. Waveform cross-correlation was performed using the entire record. Values calculated using responses with colocated sources are highlighted in bold.

		IRF: Hammer Blow Source Location								
		S_1	S_2	S_3	S_4	S_5	S_6	S_7	S_8	
Damaged Location	-	μ	0.78	0.85	0.80	0.83	0.81	0.83	0.80	0.85
		σ	0.05	0.09	0.01	0.01	0.07	0.01	0.01	0.01
		N	15	15	15	15	15	15	15	15
	S_1	μ	0.11	0.44	0.46	0.53	0.51	0.56	0.51	0.56
		σ	0.05	0.09	0.01	0.01	0.07	0.01	0.01	0.01
		N	15	15	15	15	15	15	15	15
	S_3	μ	0.52	0.50	0.41	0.48	0.44	0.51	0.51	0.51
		σ	0.01	0.01	0.02	0.01	0.01	0.01	0.01	0.01
		N	15	15	15	15	15	15	15	15
	S_5	μ	0.60	0.57	0.46	0.54	0.33	0.45	0.47	0.53
		σ	0.01	0.00	0.01	0.01	0.03	0.01	0.02	0.01
		N	15	15	15	15	15	15	15	15
S_7	μ	0.60	0.60	0.52	0.60	0.45	0.54	0.31	0.50	
	σ	0.01	0.00	0.01	0.01	0.03	0.01	0.03	0.01	
	N	15	15	15	15	15	15	15	15	

Table 2.6: **Steel Frame: Correlation Values (IRFs Before and After Damage)** IRFs were generated by using a force transducer hammer to apply an impulsive force load along the y-axis to each of the eight beam-column connections (S_1 - S_8). A total of five hammer blows were delivered at each source location. IRFs for a damaged frame were obtained by performing a tap test on the frame with a damaged beam-column connection. Damage was introduced by removing all three bolts from the connection (S_1 , S_3 , S_5 , or S_7), with the stiffness of the frame rigidly holding the beam and column in place. An impulsive hammer blow was applied to each of the eight source locations, for each of the four damaged connection cases. This was performed a total of three times. The prerecorded IRFs were cross-correlated with the response of the damaged frame to an impulsive hammer blow applied at the same source location, for each of the four damaged connection cases. Results were averaged over 15 total trials. Waveform cross-correlation was performed using the entire record. Values calculated using responses with colocated sources are highlighted in bold.

	Hammer Blow Source Location				
	15 NW (I)	15 NW (II)	15 SE (I)	15 SE (II)	3
15 NW (I)	-	0.51	0.10	0.08	0.04
15 NW (II)	0.51	-	0.10	0.09	0.05
15 SE (I)	0.10	0.10	-	0.46	0.06
15 SE (II)	0.08	0.09	0.46	-	0.05
3	0.04	0.05	0.06	0.05	-

Table 2.7: **Steel Moment-Resisting Frame Building: Correlation values (IRFs)**. A hammer blow was applied at one of three locations (near a moment-connection at the northwest corner of the 15th floor, near a moment-connection at the southeast corner, and on the third floor stairwell). Waveform cross-correlation was performed using templates with a length of 0.2 seconds. Results were stacked and normalized, so that the resulting correlation values ranged between zero and one. Colocated IRFs have the highest correlation values. The highest correlation value between the 15 NW IRFs and the 15 SE IRFs is 0.10, which is quite low considering that the IRF sources are located on the same floor. This means that it is possible to distinguish between locations within a single floor using this method. The diagonal values in the table above have been omitted, for the same source, they are all equal to one. These results could be improved if only signals with a high signal-to-noise ratio are computed in the template, or if the template is formed by stacking over multiple trials. Values calculated using responses with colocated sources are highlighted in bold.